Biochemistry (Moscow), Vol. 66, No. 6, 2001, pp. 646-657. Translated from Biokhimiya, Vol. 66, No. 6, 2001, pp. 797-810.

Isolation, Purification, and Characterization of Catalase from the Methylotrophic Yeast *Pichia pastoris*

M. V. Potapovich[1], A. N. Eryomin[1], I. M. Artzukevich[2], I. P. Chernikevich[2], and D. I. Metelitza[1]*

[1]*Institute of Bioorganic Chemistry, National Academy of Sciences of Belarus, ul. Kuprevicha 5/2, Minsk, 220141 Belarus; fax: (375)-(172) 63-7274; E-mail: enzyme@ns.iboch.ac.by*
[2]*Grodno State Medical University, ul. Gor'kogo 80, Grodno, 230015 Belarus; fax: (375)-(152) 33-5341; E-mail: artsuk@grsmi.unibel.by*

Received October 26, 2000

Abstract—Catalase (CAT_{pp}) with molecular weight 223 kD was isolated from the methylotrophic yeast *Pichia pastoris* and purified 90-fold by ion-exchange chromatography and gel filtration. Quantitative parameters of absorption and CD spectra of CAT_{pp} solutions and of its membrane-concentrated form (CAT_{pp}-conc) were studied. Rates of H_2O_2 decomposition and kinetic characteristics K_m and k_{cat} of CAT_{pp} and CAT_{pp}-conc were determined in 10 mM phosphate buffer (pH 7.4) at 30°C, as well as the effective constant k_{in} of the enzyme inactivation rate during the catalysis and the constant k_2 of the interaction rate of the Complex I catalases with H_2O_2. Thermal inactivation of CAT_{pp} in solutions at 45°C was characterized by the effective rate constant k_{in}^*, and the low-frequency (27 kHz) ultrasonic inactivation of CAT_{pp} at 20°C was characterized by the first-order rate constant k_{in}(US). All spectral and kinetic characteristics of CAT_{pp} and CAT_{pp}-conc were compared with the corresponding values for catalase from bovine liver (CAT) and for catalase from the methylotrophic yeast *Candida boidinii* (CAT_{cb}). All three catalases were rather similar in their spectral properties but strongly varied in their kinetic parameters, and their comparison suggests that CAT_{pp} should be the best enzyme in its overall properties as it displayed the maximal efficiency in terms of k_{cat}/K_m, thermal stability comparable with the thermal stability of CAT in terms of k_{in}^*, the minimal k_{in}, and high stability in the ultrasonic cavitation field at the US power of 60 W/cm^2.

Key words: catalase from the yeast *Pichia pastoris*, bovine liver catalase, absorption spectra, CD spectra, kinetics, operational stability, inactivation by cyclic process, thermal inactivation, ultrasonic inactivation

Catalase (EC 1.11.1.6) and superoxide dismutase (SOD, EC 1.15.1.1) are the main components of the protection system against toxic forms of activated oxygen $O_2^{\cdot}$ and H_2O_2 in human and animal tissues [1, 2]. The physiological significance of these enzymes is the basis for constant interest in their preparation for medical [1-3] and biotechnological [3-5] purposes. Catalase and SOD are of the group of so-called suicide biocatalysts, which lose their stability during functioning. Therefore, increasing the operational stability of catalase is an urgent problem in the development of preparations containing this enzyme together with SOD or separately.

We have suggested the use of the effective rate constant k_{in} (operational stability) as a quantitative parameter of catalase stability during its enzymatic reaction. This constant can be determined from linear anamorphoses of kinetic curves of hydrogen peroxide consumption in coordinates "$1/\ln([H_2O_2]_o/[H_2O_2]_t) - 1/t$", where t is time and $[H_2O_2]_o$ and $[H_2O_2]_t$ are the initial and instantaneous concentrations of hydrogen peroxide [6-8]. This simple method for quantitative description of operational stability of catalases was shown to be good in the characterization of both catalase itself and its various conjugates in aqueous medium [6] and in reversed micelles of surface-active substances in organic solvents [7, 8]. It seems that Unfortunately, the operational stabilities of bovine liver catalase and of its conjugates with SOD are low, their k_{in} values being in the range of $(0.2\text{-}6.2)\cdot10^{-3}$ sec^{-1} at 30°C [7, 8].

The problem of stabilization might be solved by replacement of the bovine liver enzyme, which is commonly used for production of antioxidant preparations [5-9], by more stable catalases from other natural sources. It is known that enzymes of microorganisms are often

Abbreviations: AO) alcohol oxidase; CAT) bovine liver catalase; CAT_{pp}) catalase from the yeast *P. pastoris*; CAT_{cb}) catalase from the yeast *C. boidinii*; poly(ADSNP)) poly(2-aminodisulfide-4-nitrophenol).

* To whom correspondence should be addressed.

0006-2979/01/6606-0646$25.00 ©2001 MAIK "Nauka/Interperiodica"

much more resistant than their analogs from animal tissues [10]. Quite recently eucaryotic catalase-peroxidase was for the first time isolated from *Penicillium simplicissium*: this intracellular enzyme consists of two subunits with relatively high catalase and peroxidase activities [11]. In our laboratory, together with the Institute of Microbiology, National Academy of Sciences of Belarus, extracellular catalases produced by *Penicillium* fungi *P. piceum*, *P. kapuscinskii*, and *P. varians* were for the first time isolated and purified by successive filtration of culture fluids [12]. Maximal activity higher than that of bovine liver catalase (CAT) was shown by the catalase from *P. piceum*, and its operational stability (in terms of k_{in} at 30°C) was 2-3-fold higher than that of bovine liver catalase [12]. The thermal stabilities of these fungal catalases were close to that of CAT.

Methylotrophic yeasts are promising sources of redox enzymes for biotechnology [13] because they actively synthesize alcohol oxidase (AO, EC 1.1.3.13) and the accompanying catalase that are located in specific organelles (peroxisomes) and can constitute up to 30-45% of the total soluble cell protein. We have recently isolated, purified, and kinetically characterized catalase from the methylotrophic yeast *Candida boidinii* (CAT_{cb}): this enzyme is similar to bovine liver catalase in catalase efficiency in terms of k_{cat}/K_m and 3.5-fold better in operational stability [14]. The small amount of CAT_{cb} is due to its low thermal stability that seems to be associated with the membrane origin of this biocatalyst.

So far, the isolation and characterization of new catalase forms with high catalytic efficiency and with increased operational and thermal stabilities remains an important problem for modern biotechnology and biochemistry. Therefore, the purpose of the present work was to isolate, purify, and spectrally and kinetically characterize the intracellular catalase from the methylotrophic yeast *P. pastoris* (CAT_{pp}) and to compare this enzyme with another yeast catalase (CAT_{cb}) studied previously [14] and with bovine liver catalase.

MATERIALS AND METHODS

Bovine liver catalase with optical purity index 0.61 from Fluka (Switzerland) and catalase from the yeast *P. pastoris* as a precipitate in ammonium sulfate were used. The following reagents were used: human serum albumin (HSA), dithiothreitol, DEAE-cellulose, and a reagent kit for electrophoresis (Reanal, Hungary); Sepharose 4B (Pharmacia, Sweden); DEAE-Toyopearl 650M (Toyo Soda, Japan); a set of protein markers (Amersham, USA); SDS (Serva, Germany); diluted perhydrol (Reakhim, Russia). Methanol and all other reagents were from Reakhim.

The polymeric inhibitor poly(2-aminodisulfide-4-nitrophenol) (poly(ADSNP)) was synthesized as described earlier [15] and kindly presented by Dr. Yu. P. Losev (School of Chemistry, Belorussian State University, Minsk). The poly(ADSNP) had average molecular weight ~1400 daltons and contained 6-7 monomer units.

Protein and reagent concentrations were determined spectrophotometrically with Perkin-Elmer (Sweden), Specord M 400 (Germany), and SF-46 (LOMO, Russia) devices using the following molar extinction coefficients: H_2O_2, $\varepsilon_{230} = 72.4$ [16]; catalase, ε (Soret band maximum) = $3.24 \cdot 10^5$ [17]; poly(ADSNP), $\varepsilon_{255} = 6.3 \cdot 10^4$ and $\varepsilon_{364} = 3.1 \cdot 10^4$ $M^{-1} \cdot cm^{-1}$ [18].

CD spectra of the catalases were recorded at room temperature in aqueous solutions containing 30% glycerol and 10% ethanol in 0.1-cm pathlength cuvettes with a Jasco J-20 spectropolarimeter (Japan) over the wavelength range 195-260 nm. The molar ellipticities of the catalases were calculated by the formula [19]:

$$[\theta]_\lambda = M \cdot (\pm H) \cdot S / 10d \cdot C ,$$

where M is the average molecular weight of the amino acid residue of the catalase (114.8 daltons); H the difference between the spectra intensities of the experimental and control specimens (cm); S the device sensitivity (deg/cm); d the cuvette thickness (cm); C the protein concentration (g/cm^3). The secondary structure of catalase was analyzed from the CD spectral data using the CDNN 2.1 computer program, which includes 33 reference CD spectra [20].

Isolation and purification of catalase from *Pichia pastoris*. *Yeast culture.* CAT_{pp} was isolated from *P. pastoris* F-884 from the collection of microorganisms of the Institute of Microbiology, National Academy of Sciences of Belarus (Minsk). Methylotrophic yeast cells were grown in a periodic regime on mineral medium containing in 1 liter: $(NH_4)_2SO_4$, 5 g; KH_2PO_4, 1 g; $MgSO_4$, 0.5 g; NaCl, 0.1 g. The only source of carbon was methanol (0.4 vol. %). The cells were grown at 29°C in 5-liter flasks under constant aeration at airflow rate 2 liters/min. The cell concentration was determined by the absorption of the suspension at 623 nm. The culture medium was centrifuged (3000*g*, 15 min), the cells were washed in 20 mM phosphate buffer (pH 7.6), and the suspension was centrifuged under the conditions mentioned above. The yeast biomass was frozen and stored at −10°C. All steps of isolation and purification of catalase were carried out at 4-6°C.

Preparation of cell-free extract. Thawed wet yeast biomass (10 g) was suspended in 30 ml of 10 mM Tris-HCl buffer (pH 7.6) containing 50 mM NaCl, 0.1 mM EDTA, and 0.1 mM dithiothreitol (buffer A). The suspension was supplemented with 18 g quartz sand pretreated with concentrated hydrochloric acid for 30 min. The cells were broken with an L-17 homogenizer at 1000*g* for 15 min. Whole cells and large cell fragments were removed by

centrifugation (4000*g*, 20 min), and CAT_{pp} was isolated from the supernatant fluid.

Purification of CAT_{pp} by ion-exchange chromatography. Cell-free extract containing 810 mg protein was placed onto a column (2 × 20 cm) filled with DEAE-Toyopearl 650 M and balanced with buffer A. The column was washed with 300 ml of buffer A, and proteins were eluted with a NaCl gradient (reservoir and mixer volumes 200 ml, gradient from 0.1 to 0.5 M, elution rate 16 ml/h). Similarly to the case of CAT_{cb} purification [14], fractions of CAT_{pp} gave a clear second peak after the accompanying proteins and were easily separable from a third peak that corresponded to alcohol oxidase. The fractions with the maximum activity of CAT_{pp} were combined, and the protein was precipitated with ammonium sulfate.

During the purification of CAT_{pp}, the protein was analyzed by the method of Lowry et al. [21] or spectrophotometrically by the absorption at 280 nm. The specific activity of catalase was determined at 25°C in 70 mM phosphate buffer (pH 7.0) and expressed in international units (IU) (μmol H_2O_2/min per mg protein). The first stage of purification resulted in CAT_{pp} preparation with specific activity of $15 \cdot 10^4$ IU, 16-fold higher than that in the cell-free extract.

Purification of CAT_{pp} by gel filtration. The CAT_{pp} precipitate in ammonium sulfate was dissolved in the minimal volume of buffer A and placed onto a column (1.1 × 100 cm) filled with Sepharose 4B and equilibrated with 20 mM Tris-HCl buffer (pH 7.6) containing 0.1 M NaCl. The same buffer was passed through the column at the rate of 8 ml/h. The enzyme was eluted from the column as single peak. The second stage of purification resulted in CAT_{pp} preparations with specific activity of $8.26 \cdot 10^5$ IU, nearly 90-fold higher than that of the cell-free extract.

Concentration of the CAT_{pp} solution. Aqueous solutions of CAT_{pp} containing 30% glycerol and 10% ethanol were ultrafiltered in an Amicon-3 cell (USA) using Capron filters with pore diameter of 0.2-μm (Khiiu Kalur, Estonia), of 0.45 μm (Mechta, Minsk), and PA-100 membranes (MIFIL, Minsk), with a nominal molecular weigh halting limit of 100 kD. The CAT_{pp} solution (3 ml) was concentrated successively on Capron filters and on PA-100. After filtration, the concentrate was at each stage diluted to 3 ml with aqueous solution containing 30% glycerol and 10% ethanol. At the final stage, the CAT_{pp} concentrate was diluted in 2 ml of the glycerol–ethanol solution and then centrifuged 25 min at 3500*g*. The precipitate was removed, and the supernatant fluid was used as the sample denoted as CAT_{pp}-conc.

Preparation and characterization of HSA–poly (ADSNP) complex. The complex was prepared in 0.5 mM bicarbonate buffer (pH 9.0) containing 7.1 μM HSA and 31% ethanol. The mixture of polydisufide with the protein at the ratio of 70 : 1 was kept at ~6°C for 20 h. The resulting complex was washed free of unbound polydisulfide, first with water–ethanol solution and then with distilled water, using a PAN-20 ultrafiltration membrane (MIFIL, Minsk) with protein retaining limit of 20 kD. The complex was stored at ~6°C in aqueous solution. The concentration of poly(ADSNP) bound to HSA was calculated by the difference in absorption spectra at wavelengths of 255 and 364 nm. The calculations indicated that in the complex one molecule of HSA corresponded, on average, to ~7.7 molecules of poly(ADSNP).

Determination of catalase molecular weights by electrophoresis in polyacrylamide gel in the presence of SDS. Electrophoresis of catalases was performed in buffer mixture (pH 8.9) in a Reanal Model 69 device (Hungary). The concentration of polyacrylamide gel was 7%. Protein solutions were prepared by mixing 0.14 ml of 1% SDS, 0.14 ml of 1% dithiothreitol, and 0.1 ml of catalase solution (final protein content 200 μg/ml). The samples were kept for 90 sec in a boiling water bath. The upper electrode buffer contained 0.05% SDS. Molecular weights of the catalases were determined using a set of calibration proteins (Amersham, USA).

The molecular weight of the CAT_{pp} subunit was 55.7 kD, and the enzyme preparation contained minor components of 40 and 68 kD. The molecular weight of the CAT subunit was 59.0 kD, and its preparation contained minor components of 74, 117, and 218 kD. The CAT_{pp}-conc preparation was only slightly instilled in 7% polyacrylamide gel, and, thus, had increased stability under denaturing conditions. Based on the experiments, the calculated molecular weights were 223 kD for CAT_{pp} (compared to 236 kD for CAT).

Determination of catalase catalytic activities. The specific activity of CAT_{pp} was determined at 25°C by the rate of decomposition of H_2O_2 in 70 mM phosphate buffer (pH 7.0) as described above and expressed in international units (IU).

The kinetics of H_2O_2 decomposition by catalase were determined at 30°C in distilled water or in 10 mM phosphate buffer (pH 7.4), and the decomposition of hydrogen peroxide was followed spectrophotometrically with the SF-46 spectrophotometer (LOMO, Russia) by the decrease in light absorption at 230 nm. The reference cuvette contained all components of the reaction medium except H_2O_2. The catalase activities were characterized by the initial rates of H_2O_2 decomposition (v_o, $M \cdot sec^{-1}$). From the dependences of v_o on $[H_2O_2]$ in double reciprocal coordinates, Michaelis constants (K_m, M) and catalytic constants (k_{cat}, sec^{-1}) were calculated.

Rate constants of the interaction of catalase Complex I with a second H_2O_2 molecule (k_2, $M^{-1} \cdot sec^{-1}$) and effective rate constants of catalase inactivation during the enzymatic process (k_{in}, sec^{-1}) were determined concurrently as described previously [6-8]: to do this, linear

anamorphoses of kinetic curves of H_2O_2 decomposition were plotted in coordinates $1/\ln([H_2O_2]_o/[H_2O_2]_t) - 1/t$, where t is time. The tangent of the slope in these coordinates is $1/k_2 \cdot [CAT]_o$, and the intercept on the abscissa axis is $-k_{in}$.

Thermal inactivation of catalases. Catalases were thermally inactivated at 45°C in 10 mM phosphate buffer (pH 7.4) at varied concentrations of the enzyme. The inactivation of catalases was studied at concentrations from 0.03 to 0.2 nM. At certain times during the thermal inactivation, aliquots were taken from the thermostatted protein solution and placed into a cuvette containing H_2O_2. The substrate decomposition was followed spectrophotometrically at 45°C. The residual catalase activity was characterized by the effective rate constant of H_2O_2 decomposition (k, sec^{-1}). The thermal inactivation of catalases was characterized by the first-order rate constant of inactivation (k^*_{in}, sec^{-1}), which was determined graphically from time dependences of k values in semi-logarithmic coordinates.

Effect of ultrasound (US) on catalases in solution. For generation of US, a Tekhnosonic device (Bauman Moscow High Technical College, Moscow) was used at the operating frequency of 27 kHz. The device was equipped with a piezoceramic transformer and a titanium waveguide. US with specific power (intensity) of 60 W/cm^2 was used, this corresponding to 57 μm fluctuation amplitude of the waveguide end-wall. Catalase solutions were sonicated at 20°C in 10 mM phosphate buffer (pH 7.4) at the enzyme concentration of 0.1 μM. During the US treatment, aliquots were taken, added to a cuvette containing H_2O_2, and the residual enzyme activities were determined. For each aliquot the constant of H_2O_2 decomposition (k, sec^{-1}) was determined from the semi-logarithmic anamorphoses of kinetic curves describing the decrease in the H_2O_2 concentration. The rate of US inactivation was characterized by the effective first-order inactivation constant k_{in}(US) in sec^{-1}, which was calculated from semi-logarithmic anamorphoses of changes in k values in sec^{-1} depending on the time of US treatment of the sample.

RESULTS AND DISCUSSION

The contents of *P. pastoris* peroxisomes is strongly structured. Therefore, optimal conditions are needed to provide complete separation of AO and CAT_{pp}, which are the main fraction of the peroxisome proteins. By varying the ionic strength and pH of solutions and by testing various ion-exchangers, DEAE-cellulose and DEAE-Sephadex were shown to be ineffective because they failed to separate the two enzymes. AO and CAT_{pp} could be virtually completely separated by ion-exchange chromatography only when a high-resolution DEAE-Toyopearl 650M was used. CAT_{pp} was nearly completely purified at the second stage by gel filtration.

Purification and storage are inevitably associated with aggregation of the catalase: at high concentrations, bovine liver catalase easily aggregates in aqueous solution, and this is accompanied by a decrease in the catalytic rate of H_2O_2 decomposition by the catalase. To assess the effect of CAT_{pp} aggregation on its properties, the enzyme was repeatedly concentrated on membranes with various pore diameters, and water-soluble protein aggregates were collected. The resulting sample of the aggregated enzyme (CAT_{pp}-conc) was compared to CAT_{pp} not subjected to concentration on membranes.

Spectral characteristics of CAT_{pp} are compared to the corresponding parameters of CAT and CAT_{cb} in Table 1. The absorption maximums of CAT_{pp} and CAT in the UV region are virtually the same, whereas the maximum for CAT_{pp}-conc is markedly displaced to longer wavelength. The positions of Soret band maximums vary more markedly for samples of the different catalases: 3.4-3.9 nm for CAT_{pp} and 7 nm for CAT_{cb} compared to the bovine liver catalase.

Figure 1 presents CD spectra of the catalases various concentrations in distilled water: CAT_{pp} (*1*, *2*), CAT_{pp}-conc (*3-5*), and CAT (*6-8*). The figure shows that the molar ellipticities of all of the catalases significantly depend on their concentration in water and that the concentrating of CAT_{pp} (spectra *3-5*) significantly changed the shape of the CD spectra. At high concentrations of

Table 1. Absorption spectra of catalases from bovine liver and from yeast

Enzyme	RZ	λ_{max}, nm				
Bovine liver catalase	0.61	277.2	405.0	~496	~534	620.7
Catalase from *Pichia pastoris*	0.39	277.8	408.4	~496	~540	~624
CAT_{pp}-conc	0.36	278.8 278.9	408.9 408.9	~498	~537	628.4
Catalase from *Candida boidinii*	0.36	279	412	502	542	631

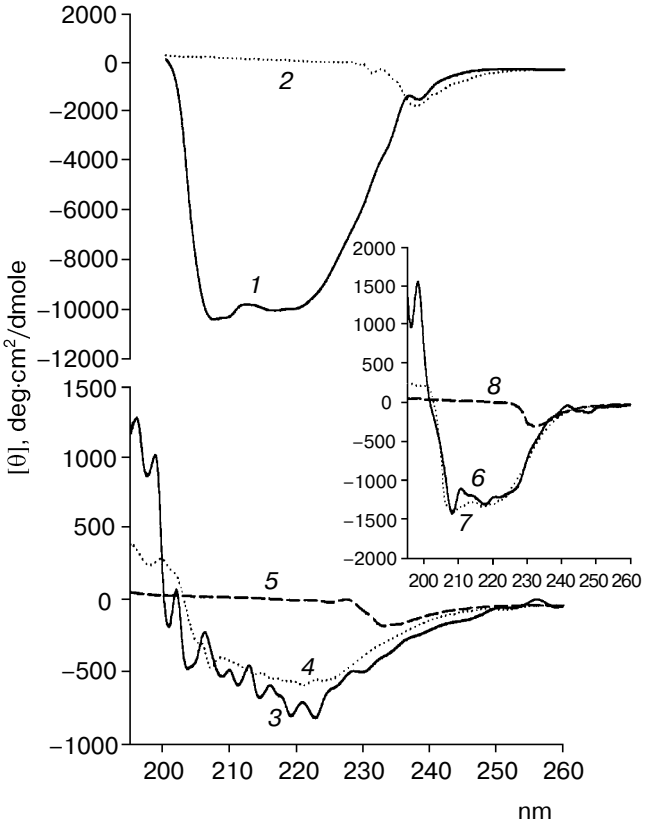

Fig. 1. CD spectra of CAT_{pp} (*1*, *2*), CAT_{pp}-conc (*3-5*), and CAT (*6-8*) in distilled water at varied concentrations of the enzymes: *1*) 1.43; *2*) 12.91; *3*) 0.57; *4*) 5.75; *5*) 57.48; *6*) 0.55; *7*) 5.50; *8*) 55.0 mg/ml protein.

the enzymes, their CD spectra were similar. On diluting the solutions, the molar ellipticity values displayed clear maximums; however, this was not found for specimens of CAT_{pp}-conc (spectra *3-5*), seemingly due to the high stability of CAT_{pp}-conc aggregations that fail to dissociate on dilution.

Elements of the secondary structure (in %) of CAT_{pp} and CAT are compared in Table 2. The contents of parallel β-sheet, β-bend, and random coil depended little on the catalase source and on their concentration in the solution. A difference was seen in the contents of α-helix and of antiparallel β-sheet, which are predominant in the concentrated catalase solutions. In the case of CAT and CAT_{pp}-conc, the contents of antiparallel β-sheet and α-helix were virtually unchanged on dilution. However, the content of α-helix strongly increases with dilution of CAT_{pp}, but this was not observed in the case of CAT. Thus, concentrations of both catalases affected their CD spectra (Fig. 1), and, correspondingly, the secondary structure of the enzymes; the contents of secondary elements in both catalases was very similar except a relatively high content of α-helix in diluted aqueous solutions of CAT_{pp} compared to CAT.

Kinetic characteristics of CAT_{pp}. Initial rate dependences of H_2O_2 decomposition at 30°C under the influence of 0.5 nM CAT_{pp} (*1*) and CAT_{pp}-conc (*2*) are presented in double reciprocal coordinates in Fig. 2: over a wide range of H_2O_2 concentrations, its decomposition follows the Michaelis–Menten equation for both CAT_{pp} samples. From the dependences shown in Fig. 2 values of K_m and k_{cat} are calculated, which are compared in Table 3. Table 3 shows that the CAT_{pp} concentration has a slight effect on the K_m values but decreases k_{cat} ~2.7-fold and the enzyme effectiveness in terms of k_{cat}/K_m nearly threefold. Thus, the aggregation of CAT_{pp} has a negative effect on its catalytic activity. It is important to compare the kinetic characteristics of CAT_{pp} with the previously determined parameters for CAT and for the other yeast catalase CAT_{cb} [14]. Table 3 shows that K_m values for CAT and CAT_{cb} are about an order of magnitude higher than the K_m for CAT_{pp}. Comparison of the catalytic constants shows that the activity of CAT is two times higher than the activity of CAT_{cb} and seven times higher than the activity of

Table 2. Contents of secondary structural elements (%) in aqueous solutions of catalases

Enzyme	[Protein], μg/ml	α-Helix	β-Sheet		β-Bend	Random coil
			antiparallel	parallel		
CAT_{pp}	12910	3.9	47.2	5.4	18.8	24.7
	1434	25.0	15.3	5.6	19.1	35.0
CAT_{pp}-conc	57480	5.1	44.9	5.4	19.0	25.6
	5748	5.1	44.7	5.4	19.0	25.8
	574.8	5.7	42.7	5.4	19.0	27.9
CAT	55000	5.1	44.9	5.4	19.0	25.6
	5500	6.3	40.4	5.4	19.1	28.8
	550	6.4	40.6	5.4	19.0	28.6

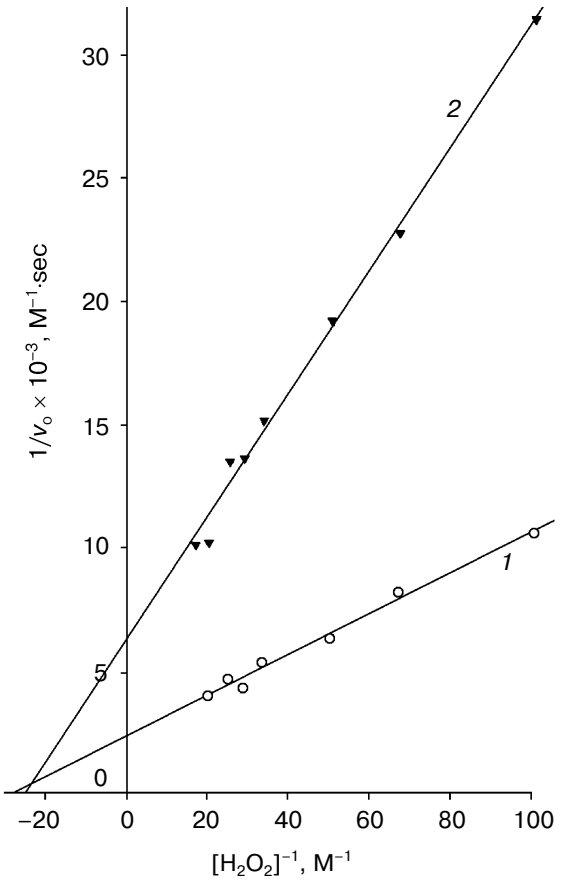

Fig. 2. Dependences in double reciprocal coordinates of the initial rate of H_2O_2 decomposition on its initial concentration in the presence of 0.5 nM catalase in 10 mM phosphate buffer (pH 7.4) at 30°C: *1*) CAT_{pp}; *2*) CAT_{pp}-conc.

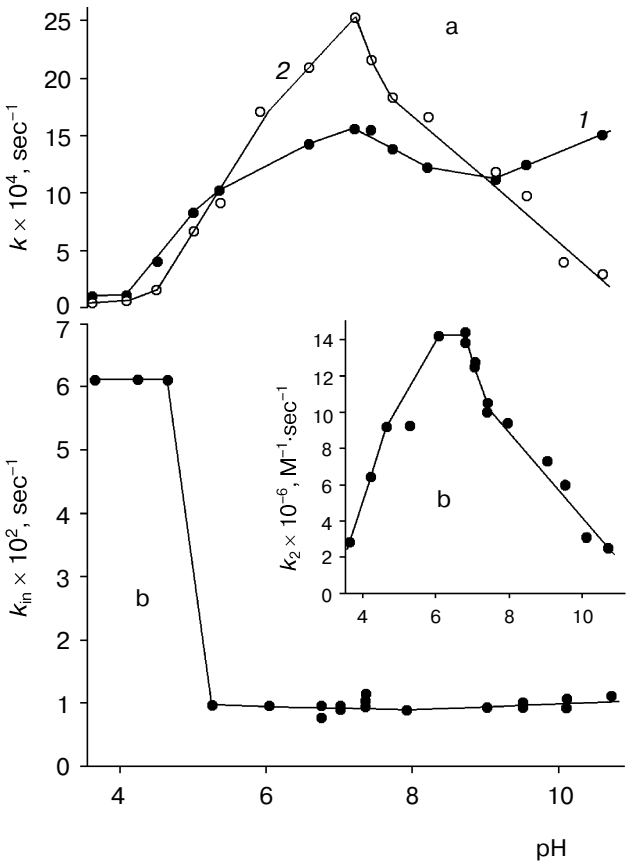

Fig. 3. Effect of pH on values of rate constants k (a) and k_{in} and k_2 (b) during the decomposition by catalase of 70 mM H_2O_2 in 20 mM citrate–phosphate (pH 3.1-7.9) and bicarbonate (pH 9.0-10.7) buffers at 30°C: a) CAT (*1*) and CAT_{pp} (*2*); b) CAT_{pp}.

Table 3. Comparison of characteristics and kinetic parameters of catalases at 30°C in 10 mM phosphate buffer (pH 7.4)

Parameter	CAT_{pp}	CAT_{cb} [14]	CAT [14]
Molecular weight, kD	223	230 ± 2	236
pH optimum	6.7-7.0	7.0-8.0	7.0-8.0
$k_{cat} \times 10^{-6}$, sec^{-1}	0.85; 0.32*	2.94-3.13	5.88
K_m, M	0.036; 0.040*	0.23	0.33
$(k_{cat}/K_m) \times 10^{-7}$, M^{-1}·sec^{-1}	2.36; 0.80*	1.36	1.78
Specific activity $\times 10^{-5}$, IU (μmol H_2O_2/min per mg)	8.26	1.43-1.52	10.1

* CAT_{pp}-conc.

CAT_{pp}. The ratios k_{cat}/K_m suggest the maximal functional activity ($2.36 \cdot 10^7$ M^{-1}·sec^{-1}) of CAT_{pp} under comparable conditions is 1.3- and 1.7-fold higher than the activities of CAT and CAT_{cb}, respectively. Data presented in Table 3 also suggest that the purification of CAT_{pp} should result in enzyme with specific activity 5.7-fold higher than that of the CAT_{cb} purified from the yeast *C. boidinii* [14].

Effect of pH on kinetic parameters of the catalases. The catalase activities are significantly affected by the pH values of the aqueous medium [22]. Therefore, we studied in detail the effect of pH on the effective rate constant of H_2O_2 consumption (k), the rate constant of CAT_{pp} inactivation during the enzymatic process (k_{in}), and the rate constant of the interaction of catalase Complex I with H_2O_2 (k_2), which is characteristic for the limiting stage of the catalase reaction [6-8, 22]. Figure 3a shows the pH dependences of rate constants k for CAT (*1*) and CAT_{pp} (*2*): the maximal rates of H_2O_2 decomposition by both catalases occur at pH 6.7-7.0. The shapes of the k vs. pH dependences for the two catalases are different only at pH > 8: the activity of CAT_{pp} decreases

Table 4. Effect of pH on the rate constants k_{in} and k_2 during the decomposition of 70 mM H_2O_2 by catalases (0.2 nM) from different sources in 20 mM citrate–phosphate (pH 4.6, 6.8) and bicarbonate (pH 9.0, 10.7) buffers

pH	CAT [14]		CAT_{pp}		CAT_{cb}	
	$k_{in} \times 10^3$, sec^{-1}	$k_2 \times 10^{-6}$, $M^{-1} \cdot sec^{-1}$	$k_{in} \times 10^3$, sec^{-1}	$k_2 \times 10^{-6}$, $M^{-1} \cdot sec^{-1}$	$k_{in} \times 10^3$, sec^{-1}	$k_2 \times 10^{-6}$, $M^{-1} \cdot sec^{-1}$
4.6	14.0	6.04	61.0	9.18	3.0	9.20
6.8	10.0	8.33	9.8	14.09	1.0	15.0
9.0	6.8	6.49	9.8	7.30	3.3	16.0
10.7	21.5	10.30	11.7	2.55		

Table 5. Kinetic parameters of catalases in the cyclic decomposition of 50 mM H_2O_2 in various media at 30°C

Enzyme/conditions	Conversion of H_2O_2, %	$k \times 10^3$, sec^{-1}	$k_{in} \times 10^3$, sec^{-1}	$k_2 \times 10^{-6}$, $M^{-1} \cdot sec^{-1}$
Bovine liver catalase (0.5 nM):				
H_2O	32.5	1.06	4.5	2.73
H_2O + 20 μM poly(ADSNP)	9.2	0.28	10.6	0.98
H_2O + HSA–poly(ADSNP)	59.3	0.83	1.5	18.00
10 mM PB (pH 7.4): 1st cycle	100	5.40	5.7	11.8
2nd cycle	6.2	0.57	40.0	
10 mM PB (pH 7.4) + 20 μM poly(ADSNP)	90.6	3.64	5.6	8.32
Catalase from *P. pastoris* (0.5 nM):				
H_2O*	~1	0.10		
H_2O	~1	0.05	9.8	0.20
H_2O + 20 μM poly(ADSNP)	~1	0.13		
10 mM PB (pH 7.4)*	26.0	1.50	3.6	3.03
10 mM PB (pH 7.4)	57.7	2.66	2.1	5.93
10 mM PB (pH 7.4) + 20 μM poly(ADSNP)	70.2	1.31	1.7	2.85

* CAT_{pp}-conc.

more sharply than the activity of CAT. Figure 3b (curve *2*) shows the pH dependence of rate constant k_2 for CAT_{pp}: the shape of this dependence is alike that of the k vs. pH dependence for CAT_{pp} (Fig. 3a, curve *2*), this being quite reasonable because the rate constant k_2 determines the course of H_2O_2 decomposition by catalase. The operational stability of CAT_{pp} expressed by the effective rate constant k_{in} (Fig. 3b) changes quite differently: in the pH range 5.2-10.7 the operational stability of CAT_{pp} is virtually unchanged and maximal (k_{in} is minimal); however, at pH < 5 the k_{in} value increases dramatically due to strong inactivation of CAT_{pp} in acidic media.

The rate constants k_{in} and k_2 at various pH values (4.6-10.7) for three catalases are presented in Table 4. The pH dependences of rate constants k_2 suggest that the maximal rate of the reaction of H_2O_2 with Complex I of different catalases should occur at different pH values: 6.8 for the yeast catalases and 10.7 for CAT. Note that the minimal values of k_{in} for the two yeast catalases are at pH ~ 6.8 along with the maximum activities of both enzymes, whereas CAT is the most stable at pH 9.0. The maximal operational stability of CAT_{cb} is observed at pH 6.8, whereas CAT_{pp} was nearly tenfold less stable under these conditions. The operational stabilities of CAT and CAT_{pp} at pH 6.8 are comparable. The maximum k_{in} value for CAT_{pp} was recorded at pH 4.6 ($61 \cdot 10^{-3}$ sec^{-1}), and this completely corresponds to the dependence presented in Fig. 3b, which shows increased lability of CAT_{pp} in acidic media.

Kinetic parameters of hydrogen peroxide cyclic decomposition by catalase are especially interesting for practice. Table 5 compares the CAT_{pp} and CAT efficiencies in the cyclic decomposition of H_2O_2 under varied conditions. Except for one case, both catalases failed to provide complete decomposition of 50 mM H_2O_2 in different media at 30°C. CAT_{pp} was especially inefficient in distilled water—the conversion of H_2O_2 was barely 1%. Addition to the solution of the effective antioxidant poly(ADSNP) [15, 18] interacting with active oxygen-containing radicals $HO^{\bullet}$ and $HO_2^{\bullet}$ did not increase the conversion of H_2O_2 above 1%. In distilled water CAT was more efficient than CAT_{pp} and provided the conversion of 32.5% of the H_2O_2. The addition of poly(ADSNP) to the reaction medium decreased to 9.2% the CAT-catalyzed conversion of H_2O_2 due to the interaction of the polydisulfide with the enzyme, decreasing the activity of the latter. We showed earlier a direct interaction of CAT with phenol polydisulfides [23].

The degree of conversion of H_2O_2 under the influence of both catalases significantly increased in phosphate buffer (pH 7.4). In the first cycle, CAT completely converted the total amount of H_2O_2 and provided the decomposition of 6.2% of the substrate in the second cycle. CAT_{pp} degraded 57.7% H_2O_2 at pH 7.4. Note that the presence of poly(ADSNP) in the solution was favorable for the effect of CAT_{pp} and increased the H_2O_2 conversion in the first cycle to 70.2%, i.e., 1.2-fold, whereas the same antioxidant decreased 1.2-fold the H_2O_2 conversion by CAT (Table 5).

The HSA–poly(ADSNP) complex containing 7.7 poly(ADSNP) molecules firmly bound to one HSA molecule was a significantly more efficient antioxidant. Indeed, in the presence of this complex in water the H_2O_2 conversion by CAT increased to 59.3% compared to 9.2% in the presence of the free antioxidant, i.e., increased 6.4-fold. Determination of the rate constants k_2 and k_{in} during the cyclic decomposition of H_2O_2 clearly confirms the previously obtained dependences and suggests quite definite conclusions.

Table 5 shows that in distilled water poly(ADSNP) (20 μM) decreased ~2.4-fold the operational stability of CAT (increase in k_{in}). The use of poly(ADSNP) complex with HSA decreased threefold the k_{in} value, i.e., increased threefold the operational stability of CAT, this resulting in enhanced conversion of H_2O_2. The interaction of poly(ADSNP) with CAT in phosphate buffer (pH 7.4) was insignificant; therefore, the k_{in} values in the presence and absence of the antioxidant were similar.

The maximum operational stability of CAT_{pp} in phosphate buffer (pH 7.4) was provided by the presence of poly(ADSNP) ($k_{in} = 1.7 \cdot 10^{-3}\ sec^{-1}$), whereas the maximum stability of CAT under these conditions was provided in the presence of the HSA–poly(ADSNP) complex ($k_{in} = 1.5 \cdot 10^{-3}\ sec^{-1}$).

Figure 4 presents the effect of increasing concentrations of poly(ADSNP) in the medium on the rate constants k, k_{in}, and k_2 during the decomposition of H_2O_2 by CAT (30°C). In water (*1*) the value of k_{in} increased directly proportional to the antioxidant concentration and did not depend on it in phosphate buffer (*2*). With an increase in the poly(ADSNP) concentration in both media, the rate constant k_2 decreased monotonically due to direct interaction of the antioxidant with CAT [23].

Thus, during the decomposition of H_2O_2 both CAT_{pp} and CAT were characterized by high values of the rate constant k_{in} (Table 5); however, they could be significantly stabilized by the antioxidant poly(ADSNP) and by the HSA–poly(ADSNP) complex, respectively. Concentrating CAT_{pp} decreased its operational stability 1.7-fold and thus decreased the level of H_2O_2 conversion 2.2-fold (Table 5).

Thermal stability of the catalases. Figure 5 presents semi-logarithmic anamorphoses of kinetic curves describing changes in kinetic activity expressed by con-

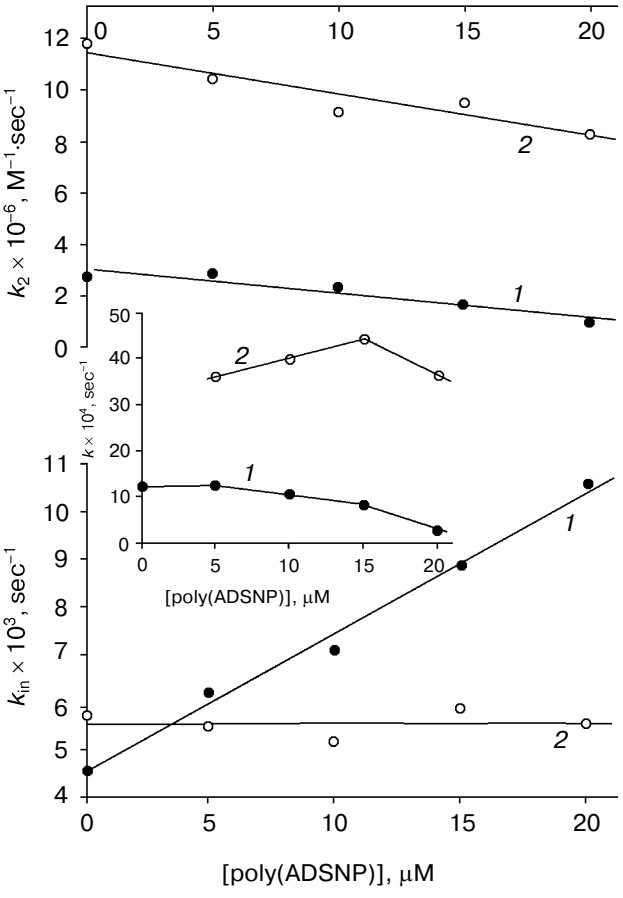

Fig. 4. Effect of the initial concentration of poly(ADSNP) on rate constants k, k_{in}, and k_2 during the decomposition of 50 mM H_2O_2 by CAT (0.5 nM) in distilled water (*1*) and in 10 mM phosphate buffer (pH 7.4) (*2*).

stants k of H_2O_2 decomposition at 45°C for CAT_{pp} (*1*, *2*) and CAT (*3*, *4*) at their concentrations in phosphate buffer (pH 7.4) 0.03 (*1*, *3*) and 0.20 nM (*2*, *4*). For both concentrations of CAT_{pp}, the dependences are characterized by a break that represents two phases of thermal inactivation, fast and slow. Under similar conditions thermal inactivation of CAT displayed no such two phases, since there are no breaks in the ln k vs. time dependences.

The effective rate constants of thermal inactivation of many oligomeric enzymes including catalase are known to depend on the protein concentration in solution [24, 25]. Therefore, we studied the thermal inactivation of both catalases at 45°C over a wide range of the enzyme concentrations (from 0.03 to 0.20 nM). In all cases, from the kinetic curves values of effective rate constants k_{in}^* of thermal inactivation were calculated for the first and second stages of the process. Figure 6 shows dependences of the inverse values k_{in}^* on the initial concentrations of CAT_{pp} (*1*, *2*) and CAT (*3*). The dependences are complicated, with breaks in the straight lines; this suggests the existence of two catalase pools with different association degree at low and high concentrations of the enzymes. Extrapolation of the linear dependence *1* for CAT_{pp} from the concentration 0.15 nM to zero provides an estimate for the effective rate constant of thermal inactivation when protein–protein interactions are minimal. The extrapolation gave effective rate constants of thermal inactivation for CAT_{pp} of $1.11 \cdot 10^{-3}$ sec^{-1} and $3.23 \cdot 10^{-4}$ sec^{-1} for the first and the second stages of the process, respectively. The first stage of thermal inactivation of CAT under conditions of infinite dilution is characterized by the rate constant $7.75 \cdot 10^{-4}$ sec^{-1}. Comparison of rate constants of the first stage suggests that CAT should be 1.4-fold more stable than CAT_{pp}. We compared earlier the thermal stability of CAT and CAT_{cb} at 55°C [12]: CAT was more than 500 times more stable than CAT_{cb}. Thus, yeast catalases have lower thermal stability than CAT, although the thermal stabilities of CAT and CAT_{pp} are comparable, whereas CAT_{cb} is anomalously unstable. Figure 7 presents effective rate constants of thermal inactivation of CAT_{pp} during the first (*1*) and the second (*3*) stages and of CAT in the first stage (*2*). Clearly, over the wide range of initial concentrations CAT is more stable than CAT_{pp}.

It is important to know how kinetic characteristics k_{in} and k_2 change during the thermal inactivation of the enzyme. Figure 8 presents linear anamorphoses of kinet-

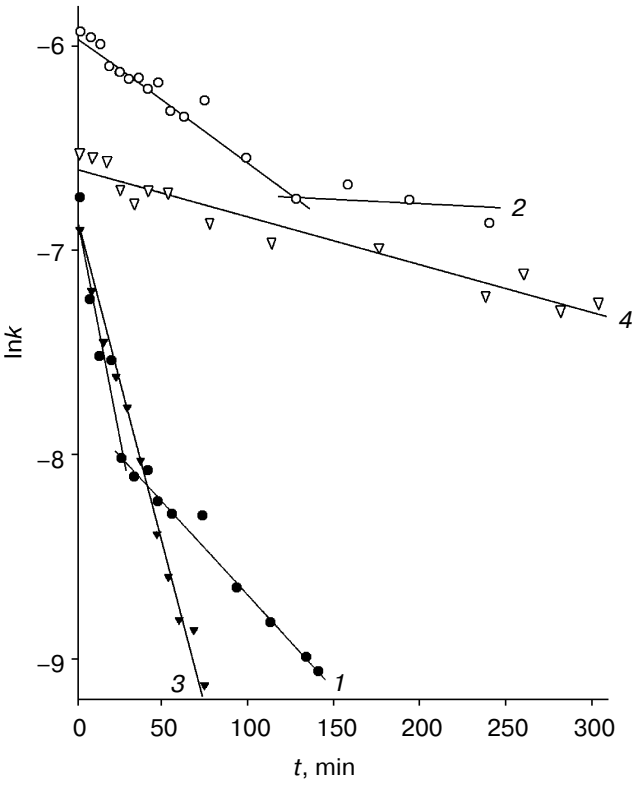

Fig. 5. Time dependences in semi-logarithmic coordinates of the effective rate constants k of decomposition of 48.3 mM H_2O_2 in 10 mM phosphate buffer (pH 7.4) at 45°C under the influence of CAT_{pp} (*1*, *2*) and CAT (*3*, *4*) at initial concentrations of both enzymes 0.03 (*1*, *3*) and 0.20 nM (*2*, *4*).

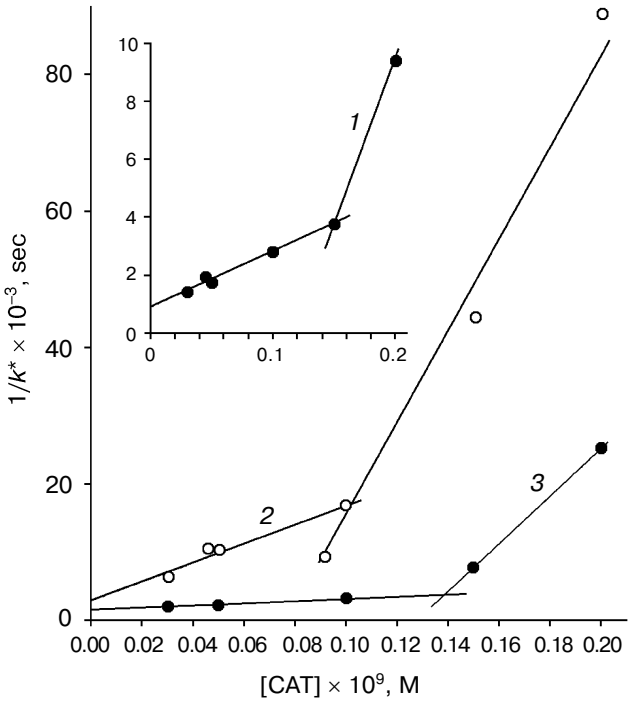

Fig. 6. Dependences of inverse values of effective rate constants of thermal inactivation of CAT_{pp} (*1*, *2*) and CAT (*3*) on the initial concentrations of the enzymes in 10 mM phosphate buffer (pH 7.4, 45°C, 48.3 mM H_2O_2): *1*, *3*) the first, and *2*) the second stages of thermal inactivation of the catalases.

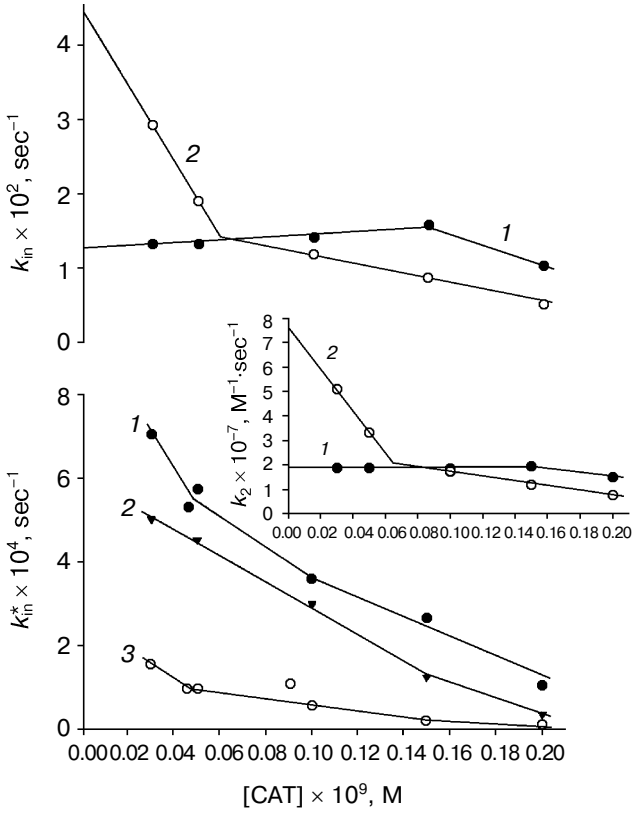

Fig. 7. Dependences of rate constants k_{in}, k_{in}^*, and k_2 during the decomposition of 48.3 mM H_2O_2 in 10 mM phosphate buffer (pH 7.4, 45°C) on the initial concentrations of CAT_{pp} (*1*, *3*) and CAT (*2*): *3*) dependence of k_{in}^* during the second stage of thermal inactivation of CAT_{pp}.

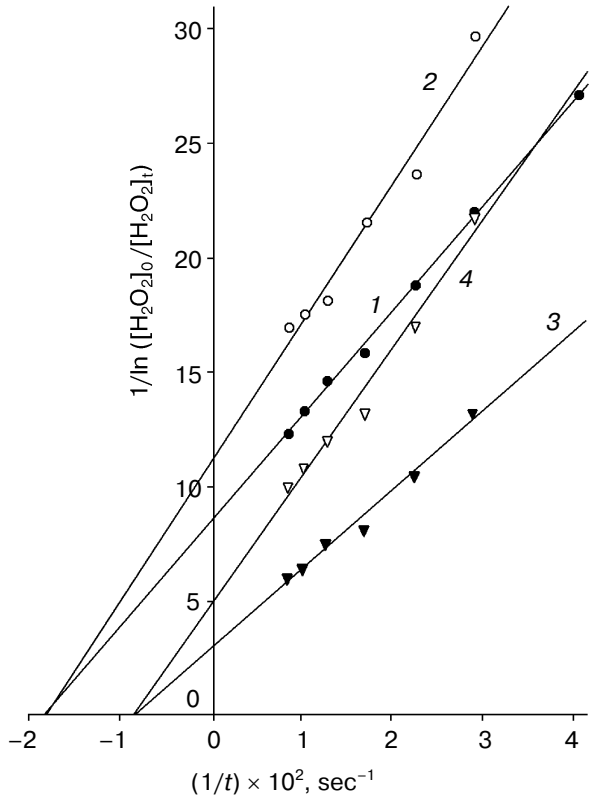

Fig. 8. Linear anamorphoses of kinetic curves of decomposition of 48.3 mM H_2O_2 in 10 mM phosphate buffer (pH 7.4) at 45°C in the presence of 0.05 nM CAT (*1*, *2*) and 0.15 nM CAT (*3*, *4*) that was pretreated at 45°C without H_2O_2 for 1 min (*1*, *3*) and for 24 min (*2*, *4*).

ic curves of H_2O_2 decomposition by CAT (initial concentrations 0.05 and 0.15 nM) thermally pretreated at 45°C for 1 min (*1*, *3*) and for 24 min (*2*, *4*). The figure shows that the thermal pretreatment of the enzyme had virtually no effect on k_{in} values (the intercepts on the abscissa did not change with CAT concentration), while the slope of the curves significantly increased reflecting changes in k_2 and in the active concentration of CAT (the slope angle tangent is $1/k_2 \cdot [CAT]_o$). Table 6 gives for comparison kinetic parameters of thermally pretreated catalases from different sources: the findings of the present work for CAT_{pp} and CAT and the earlier results for CAT_{cb} and catalase from *Penicillium piceum* [12, 14]. Table 6 shows that the thermal pretreatment of the catalases for 25, 34, and even 315 min did not change the values of k_{in}, which depended only on temperature and the catalase source and concentration. The rate constants k_2 were determined only for short-term thermal pretreatment (0.5-1 min) because in the case of prolonged heating it would be difficult to evaluate the content of catalytically active CAT due to increasing inactivation of the enzyme. Dependences of k_{in} and k_2 on the enzyme concentrations are compared in Fig. 7 for CAT_{pp} (*1*) and CAT (*2*): both rate constants were virtually unchanged with changes in the CAT_{pp} concentration, but both constants increased with decreasing CAT concentration <0.06 nM. It seems that aggregation of CAT at concentrations above 0.06 nM decreased the operational inactivation of the enzyme and its reactivity to H_2O_2 molecules (decrease in the rate constant k_2). A record value ($7.72 \cdot 10^7$ $M^{-1} \cdot sec^{-1}$) of k_2 is obtained for CAT at 45°C, this being consistent with literature data obtained for CAT by other methods [22].

Ultrasonic inactivation of 0.1 μM CAT, CAT_{pp}, and CAT_{pp}-conc by US with frequency of 27 kHz and high specific power (60 W/cm^2) in 10 mM phosphate buffer (pH 7.4) for 300-350 min follows the first-order reaction law. CAT_{pp}-conc had the lowest stability under conditions of ultrasonic cavitation, with the effective constant of inactivation rate $k_{in}(US) = 2.75 \cdot 10^{-5}$ sec^{-1}, whereas for CAT under the same conditions $k_{in}(US) = 3.9 \cdot 10^{-6}$ sec^{-1}. In the US cavitation field CAT was nearly 7-fold more stable than CAT_{pp}-conc. It is known that the cavitation-induced inactivation of proteins (enzymes) is significantly caused by free radicals HO$^\bullet$

Table 6. Kinetic characteristics of H_2O_2 decomposition in 10 mM phosphate buffer (pH 7.4) by catalases from different sources that were previously maintained for different time at 45 or 55°C

Conditions	Catalase concentration, nM	Time, min	$k \times 10^3$, sec^{-1}	$k_{in} \times 10^3$, sec^{-1}	$k_2 \times 10^{-6}$, $M^{-1} \cdot sec^{-1}$
Bovine liver catalase, 48.3 mM H_2O_2, 45°C	0.03	1	1.01	29.2	77.25
		22.5	0.49	29.2	
	0.05	1	1.30	19.0	44.13
		24	0.79	19.0	
		33.7	0.30	19.0	
	0.15	1	2.10	8.5	19.54
		23.5	1.33	8.5	
59.3 mM H_2O_2, 55°C	0.4	0	6.15	7.0	15.90
		315	4.97	7.0	
Catalase from *C. boidinii*, 59.3 mM H_2O_2, 55°C	0.4	0	4.77	2.5	13.89
		3	0.16	2.5	
Catalase from *P. pastoris*, 48.3 mM H_2O_2, 45°C	0.05	1	1.44	13.1	30.05
		25.4	0.75	13.1	
	0.15	1	2.37	15.7	22.70
		24.7	1.63	15.7	
Catalase* from *P. piceum*, 50.0 mM H_2O_2, 45°C	35 ng/ml	0.5	0.95	4.8	
		25	0.89	4.8	

* The catalase-containing culture fluid was used.

and $HO_2^{\cdot}$ produced in aqueous solutions in the cavitation zone: these radicals attack amino acid residues of protein active sites and inactivate them [26-28]. Amino acid residues of the active site of CAT_{pp}-conc are obviously more accessible to active radicals than those of CAT. However, both catalases were relatively stable to low-frequency US, whereas other oligomeric enzymes are rapidly inactivated in the US cavitation field: for urease at 37°C $k_{in}(US) = 3.3 \cdot 10^{-5}\,sec^{-1}$ and for glucose-6-phosphate dehydrogenase at 35°C, $k_{in}(US) = 1.3 \cdot 10^{-4}\,sec^{-1}$ [28].

Based on the experimental findings of the present work for CAT_{pp} and CAT and on the earlier data for CAT_{cb} and CB [14], the characteristics of the two yeast catalases and bovine liver catalase can be compared. The absorption spectra of the three catalases are generally similar; however, the Soret band maximums of yeast catalases are 3.4-7.0 nm displaced to longer wavelengths (Table 1). The CD spectra of the three catalases are strongly dependent on the enzyme concentrations and on the concentration procedure for CAT_{pp}: contents of the secondary structural elements of catalase are generally similar except for an increase in the α-helix content of CAT_{pp} on dilution (Table 2). The molecular weights of the three catalases are rather similar and vary within the limits 223-236 kD (Table 3).

The kinetic characteristics of the three catalases are different (Table 3). The K_m of CAT_{pp} is an order of magnitude lower than those of the two other catalases, and the catalytic constants of the yeast catalases are a little lower than that of CAT. Under optimal conditions the maximum efficiency expressed as k_{cat}/K_m [29] is $2.36 \cdot 10^7\,M^{-1} \cdot sec^{-1}$ for CAT_{pp}. Maximal operational stability (minimal k_{in}) is shown for CAT_{cb}, while CAT_{pp} and CAT are comparable in this parameter. The rate constants k_2 for the three catalases depend on pH and are comparable for the yeast catalases at pH 6.8 (Table 4).

The operational stability of CAT_{pp} in the cyclic decomposition of H_2O_2 can be significantly increased by addition of the polymer antioxidant poly(ADSNP) to 10 mM phosphate buffer (pH 7.4); the operational stability of CAT can be increased in the presence of the complex of this phenol polydisulfide with human serum albumin (Table 5). CAT and CAT_{pp} stabilized by the antioxidants displayed the maximum stability (minimum k_{in} $(1.5\text{-}1.7) \cdot 10^{-3}\,sec^{-1}$ at 30°C) (Table 5).

The thermal stability of CAT_{cb} is anomalously low compared to the stability of the two other catalases, CAT and CAT_{pp}, which are comparable in this parameter (Fig. 7) at different concentrations of the enzymes.

Thus, CAT_{pp} is the best enzyme in its overall physicochemical properties and kinetic characteristics, whereas CAT_{cb} is markedly inferior to the two other catalases in thermal stability. The comparative characterization of the catalases has shown that CAT_{pp} is promising for various applications and can replace bovine liver catalase because the methylotrophic yeast is a readily available and inexpensive raw material and the isolation and purification of the catalases from it is easier and less expensive than similar procedures for bovine liver catalase.

The authors are grateful to Dr. Yu. P. Losev (Belorussian State University, Minsk) for providing poly(ADSNP). This work was performed in part with support from the INTAS program (Brussels, Belgium), grant No. 99-1768, and project X99-071 of the Belorussian Foundation for Basic Research.

REFERENCES

1. Maksimenko, A. V. (1993) *Usp. Sovr. Biol.*, **113**, 361-365.
2. Maksimenko, A. V., Grigor'eva, E. L., Morozkin, A. D., Tishchenko, E. G., Minkovskii, E. B., and Torchilin, V. P. (1991) *Biokhimiya*, **56**, 1330-1336.
3. Larionova, N. I., and Torchilin, V. P. (1983) *Chemical Enzymology* [in Russian] (Berezin, I. V., and Martinek, K., eds.) MGU Publishers, Moscow, pp. 115-153.
4. Vasudevan, P. T., and Weiland, R. H. (1990) *Biotechnol. Bioeng.*, **36**, 783-789.
5. Miroshnichenko, O. S. (1992) *Biopolim. Kletka*, **8**, 3-25.
6. Eryomin, A. N., Litvinchuk, A. V., and Metelitza, D. I. (1996) *Biochemistry (Moscow)*, **61**, 483-494.
7. Eryomin, A. N., and Metelitza, D. I. (1996) *Biochemistry (Moscow)*, **61**, 1182-1192.
8. Eryomin, A. N., and Metelitza, D. I. (1997) *Prikl. Biokhim. Mikrobiol.*, **33**, 367-376.
9. Eryomin, A. N., and Metelitza, D. I. (1995) *Bioorg. Khim.*, **21**, 580-586.
10. Priest, F. G. (1987) *Extracellular Enzymes* [Russian translation], Mir, Moscow.
11. Truaije, M. W., Roubroeks, H. P., Hagen, W. R., and van Berkel, W. (1996) *Eur. J. Biochem.*, **235**, 192-198.
12. Eryomin, A. N., Mikhailova, R. V., and Metelitza, D. I. (2000) *Prikl. Biokhim. Mikrobiol.*, **36**, 221-226.
13. Veenhuis, M., and Goodman, J. (1990) *J. Cell Sci.*, **96**, 583-590.
14. Metelitza, D. I., Eryomin, A. N., Artzukevich, I. M., and Chernikevich, I. P. (1997) *Biochemistry (Moscow)*, **62**, 377-385.
15. Losev, Yu. P., Losev, V. I., Shonorov, V. I., Ivanina, N. I., and Lebedev, V. T. (1989) *USSR Author's certificate* No. 1621484, MKI C 08, L 23/06, C 08 K 5/37.
16. Nikolskii, B. P. (ed.) (1967) *A Handbook on Chemistry* [in Russian], Vol. 4, Khimiya, Leningrad, p. 919.
17. Miyhara, T., Takeda, A., Hashimori, A., and Samejima, T. (1978) *J. Biochemistry*, **84**, 1267-1276.
18. Karasyova, E. I., Nikiforova, T. V., Losev, Yu. P., and Metelitza, D. I. (1999) *Bioorg. Khim.*, **25**, 665-672.
19. Freifelder, D. (1980) *Physical Biochemistry* [Russian translation], Mir, Moscow, pp. 450-480.
20. Bohm, G. *CD Spectra Deconvolution*. CDNN2.1 // Web:http//bioinformatik.biochemtech.unihalle.de/cdnn
21. Lowry, O. H., Rosebrough, N. J., Farr, A. L., and Randall, R. J. (1951) *J. Biol. Chem.*, **193**, 265-278.
22. Pratt, J. M. (1978) in *Techniques and Topics in Bioinorganic Chemistry* (McAuliffe, C. A., ed.) [Russian translation], Mir, Moscow, pp. 194-228.
23. Eryomin, A. N., Losev, Yu. P., and Metelitza, D. I. (2000) *Biochemistry (Moscow)*, **65**, 250-258.
24. Poltorak, O. M., Chukhrai, E. S., and Torshin, I. Yu. (1998) *Biochemistry (Moscow)*, **63**, 303-311.
25. Metelitza, D. I., and Eryomin, A. N. (1987) *Usp. Khim.*, **56**, 1921-1948.
26. Margulis, M. A. (1995) *Sonochemistry and Cavitation*, Gordon and Breach, Luxemburg.
27. Klibanov, A. M., Martinek, K., and Berezin, I. V. (1974) *Biokhimiya*, **39**, 878-887.
28. Puchkaev, A. V., Tarun, E. I., Adzerikho, I. E., Mrochek, A. G., Minchenya, V. T., and Metelitza, D. I. (2000) *Izv. NAN Belarusi. Ser. Khim. Nauk*, No. 4, 70-76.
29. Berezin, I. V., and Varfolomeev, S. D. (1979) *Biokinetics* [in Russian], Nauka, Moscow, pp. 65-73.